Electronic Supplementary Material (ESI) for CrystEngComm.

Supporting Information for

Revealing the order–disorder type phase transition mechanism in two new supramolecular clathrates

Wen-Juan Wei,*[ab] Hong-Qiang Gao,[a] Ming Fang,*[a] Yun-Zhi Tang[b] and Yen Wei*[a]

EXPERIMENTAL SECTION

Synthesis. All the reagents and solvents used were of commercially available quality. **1** and **2** was obtained by slow evaporation of a solution of mixed methanol solution (10 mL) containing nortropine (1 mmol, 0.130 g), 18-crown-6 (1 mmol, 0.264 g) and perchloric acid or tetrafluoroborate acid (1 mmol) at room temperature. The large colorless block single crystals of **1** and **2** were obtained after about 2 weeks.

Powder X-ray diffraction. Room temperature powder X-ray diffraction (PXRD) experiments of **1** and **2** were performed on a Rigaku D/MAX 2000 PC X-ray diffraction instrument with Cu radiation ($K_{\alpha1}$=1.54060 Å, $K_{\alpha2}$=1.54443 Å). Variable temperature PXRD experiments of **1** and **2** were carried out on a Brucker D8 Discovery diffractometer with Cu radiation ($K_{\alpha1}$=1.54060 Å, $K_{\alpha2}$=1.54443 Å). The data were collected in the temperature range 298-445 K for θ range from 5 to 70^{o}.

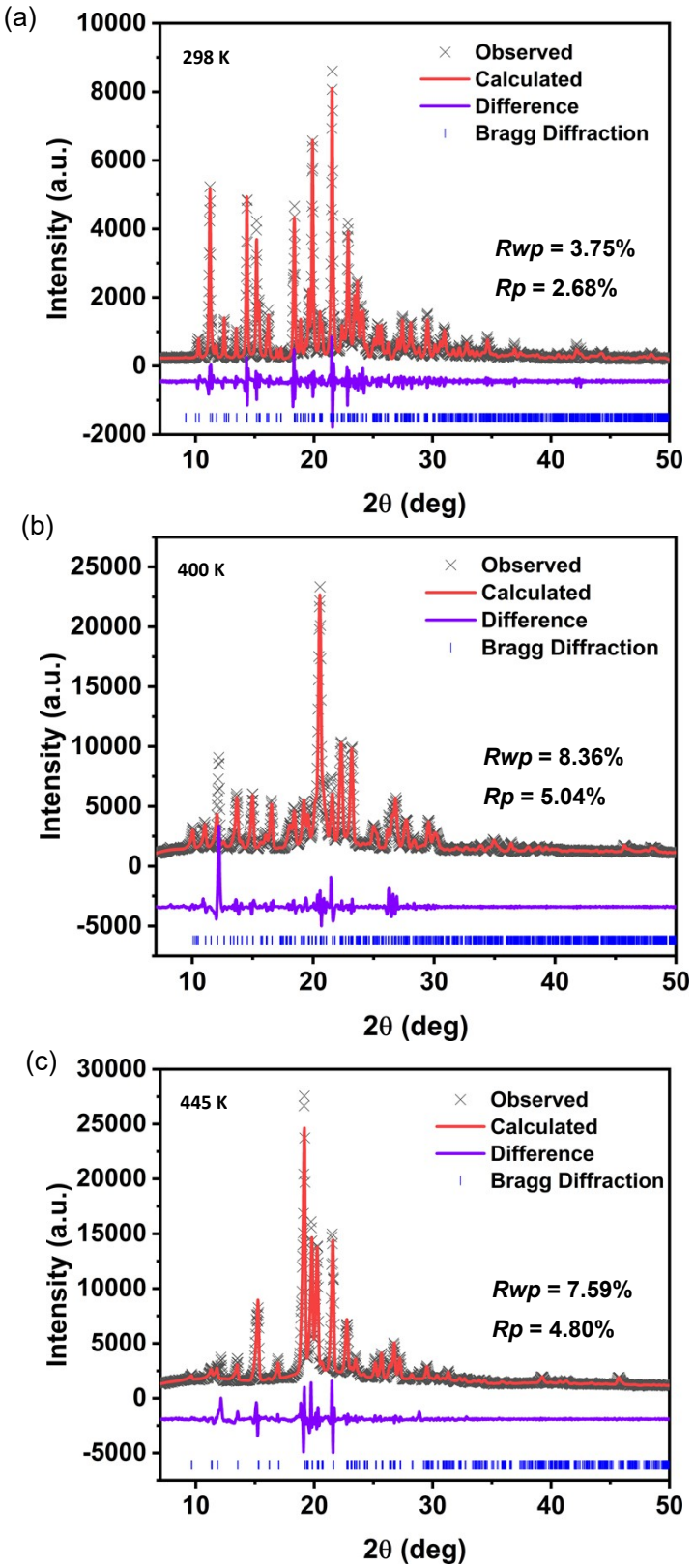

Figure S1. Patterns of the powder X-rays diffraction (PXRD) and simulated ones from the single-crystal structures of **1** at 298, 400 and 445 K.

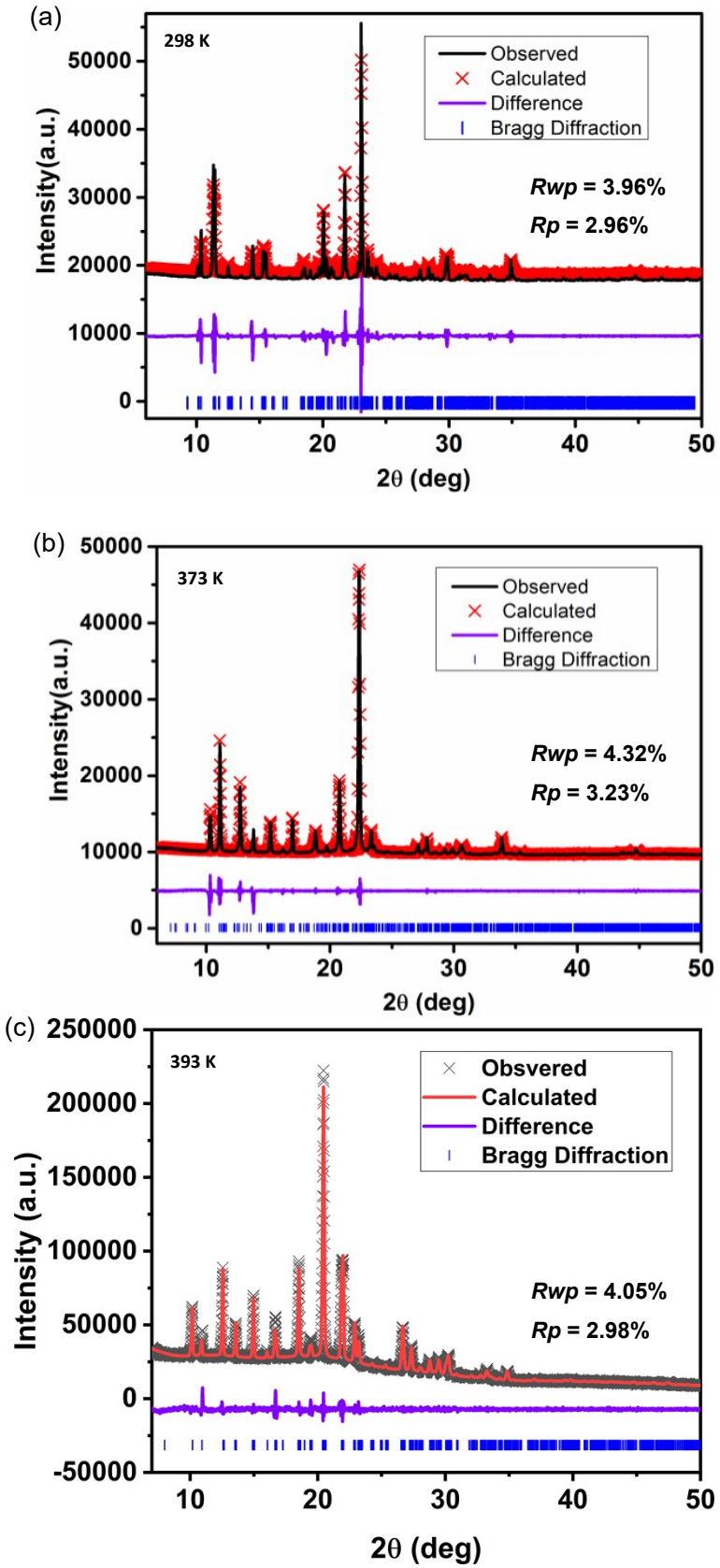

Figure S2. Patterns of the powder X-rays diffraction (PXRD) and simulated ones from the single-crystal structures of **2** at 298 K (a), 373 K (b) and 393 K (c) high-temperatures. The PXRD patterns matches very well the patterns simulated from the single-crystal structures.

DSC and TGA. Differential scanning calorimetry (DSC) measurements were conducted using a TA Q2000 DSC instrument. The DSC runs were recorded on cooling and on heating the powdered sample at the rate of temperature changes of 10 K/min. Indium standard was used for the temperature and enthalpy calibration. Thermogravimetric analysis (TGA) measurement was performed on a TA-Instruments STD2960 system from room temperature to 1050 K in nitrogen atmosphere at a rate of 10 K/min (Figure S3), indicating that **1** and **2** can be stable up to 453 K and 423 K when a dehydration process occurs.

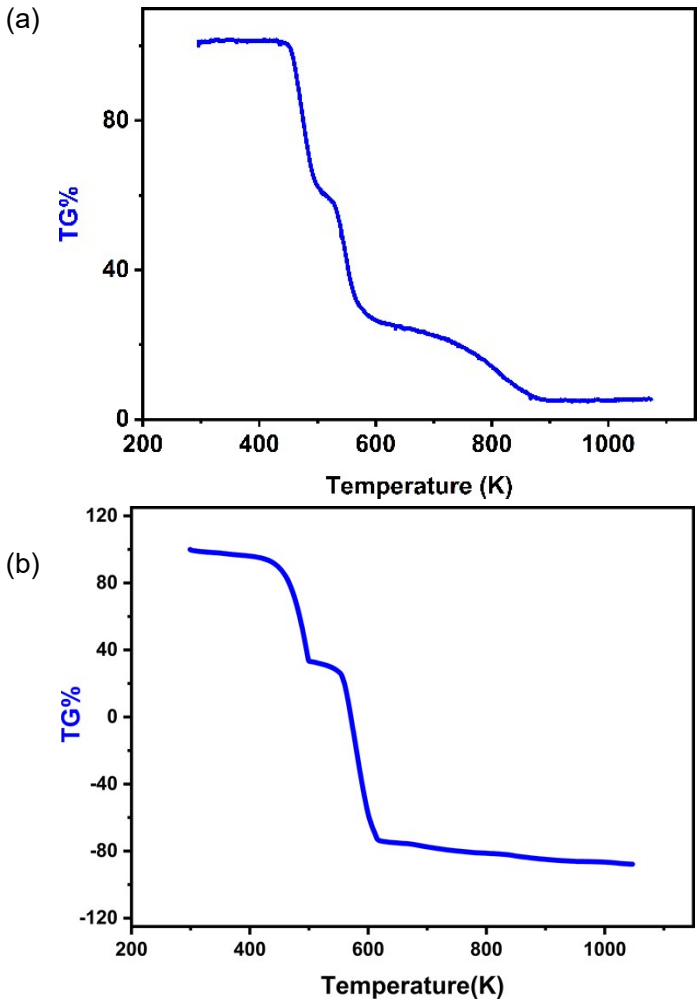

Figure S3. The thermogravimetric analysis of **1** (a) and **2** (b) in the range of 300-1050 K.

Single Crystal X-ray Diffraction. Single crystal X-ray diffractions were carried out with graphite monochromated Mo radiation (λ = 0.71073 Å) on an Oxford Diffraction Gemini E Ultra diffractometer. Data sets were collected by using *CrysAlis*^{Pro} software. The program Olex2-1.2 was employed as an interface to invoke program SHELXS97 and SHELXL97 executables.[1] The crystal structures were solved by direct methods with SHELXS97 and refined by full-matrix least squares on F^2 with anisotropic atomic displacement parameters for all non-hydrogen atoms using SHELXL97.[2, 3] All H atoms were located from molecular geometric calculations and refined with isotropic temperature parameters. The crystallographic information of **1** and **2** crystal structures were listed in the Table S1. These data can be obtained free of charge from the Cambridge Crystallographic Data Centre (CCDC) via www.ccdc.cam.ac.uk/data_request/cif (CCDC 2203857-2203862).

Table S1. Crystal data and structure refinement details for **1** at 200, 300, 365 K and **2** at 173, 293, 350 K, respectively. The crystal data of **2** at 373.15 K are refined from the corresponding high-temperature powder X-rays diffraction.

Crystal	**1** (LTP)	**1** (LTP)	**1** (LTP)	**2** (LTP)	**2** (RTP)	**2** (RTP)	**2** (HTP)
Empirical	$C_{19}H_{38}Cl$	$C_{19}H_{38}ClNO_1$	$C_{19}H_{38}ClNO_1$	$C_{19}H_{38}BF_4NO$	$C_{19}H_{38}BF_4NO$	$C_{19}H_{38}BF_4NO$	$C_{19}H_{38}BF_4NO$
Formula weight	491.95	491.95	491.95	479.31	479.31	479.31	479.31
Crystal system	orthorho	orthorhombic	orthorhombic	orthorhombic	orthorhombic	orthorhombic	orthorhombic
Space group	*Pbca*	*Pbca*	*Pnma*	*Pbca*	*Pbca*	*Pbca*	*Pnma*
Temperature (K)	200.04(1	300.00(10)	365.01(11)	173.00(10)	300.80(10)	350(2)	373.15(2)
a / Å	17.1801(	17.3155(8)	15.6730(17)	17.1067(7)	17.2870(6)	17.3460(16)	17.1726
b / Å	15.4816(	15.6324(9)	10.8757(9)	15.3661(7)	15.6308(5)	15.8138(15)	15.8594
c / Å	17.8001(	17.8689(9)	14.2780(15)	17.6923(8)	17.7593(6)	17.7610(20)	17.5853
α / °	90	90	90	90	90	90	90
β / °	90	90	90	90	90	90	90
γ / °	90	90	90	90	90	90	90
V / Å^3	4734.4(2	4836.8(4)	2433.8(4)	4650.7(4)	4798.7(3)	4872.0(8)	4789.3
Z	8	8	4	8	8	8	4
ρ / g cm^{-3}	1.380	1.351	1.343	1.369	1.327	1.307	-
μ / mm^{-1}	0.219	0.215	0.213	0.121	0.117	0.115	-
GOF on F^2	1.049	1.025	2.479	1.028	1.069	0.834	-

R_1, $[I > 2\sigma(I)]$[a]	0.0383	0.0579	0.2497	0.0477	0.0557	0.1044	-
wR_2, $[I > 2\sigma(I)]$[b]	0.0986	0.1759	0.6590	0.1089	0.1751	0.3211	-

[a] $R_1 = \Sigma||F_o|-|F_c||/\Sigma|F_o|$ [b] $wR_2 = \{\Sigma[w(F_o^2 - F_c^2)^2]/ \Sigma[w(F_o^2)^2]\}^{1/2}$

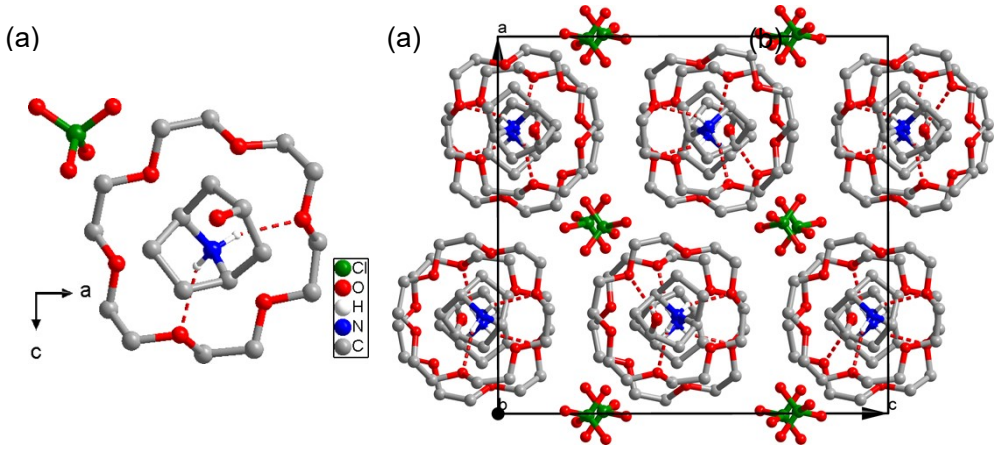

Figure S4. (a) Asymmetric units of **1** in the disordered structure of Low-temperature phase at 200 K. Dashed lines represent hydrogen bonds N–H···O. (b) The crystallographic packing diagrams of **1** viewed along the *c*-axis. Hydrogen atoms bonded to the C atoms were omitted for clarity. Dashed lines represent hydrogen bonds N–H···O and O–H···O.

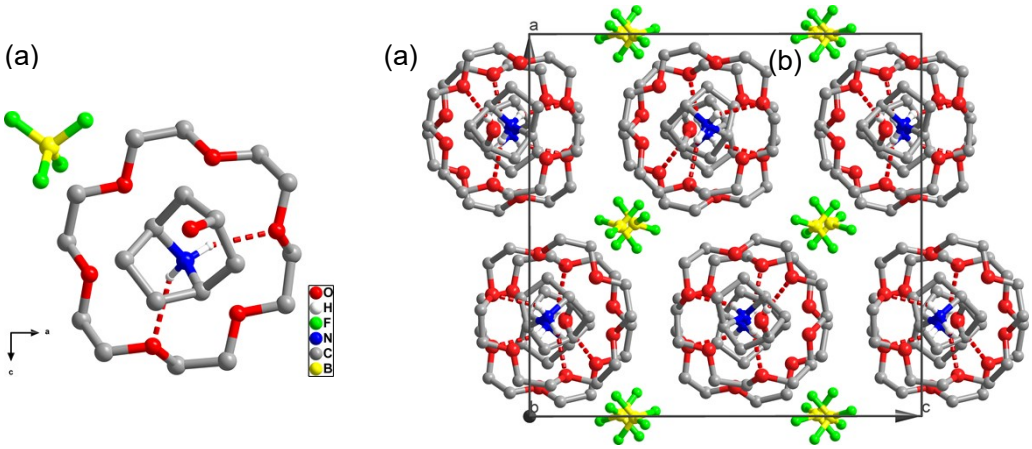

Figure S5. (a) Asymmetric units of **2** in the disordered structure of Low-temperature phase at 350 K. Dashed lines represent hydrogen bonds N–H···O. (b) The crystallographic packing diagrams of **2** viewed along the *c*-axis in the LTP at 350 K. Hydrogen atoms bonded to the C atoms were omitted for clarity. Dashed lines represent hydrogen bonds N–H···O and O–H···O.

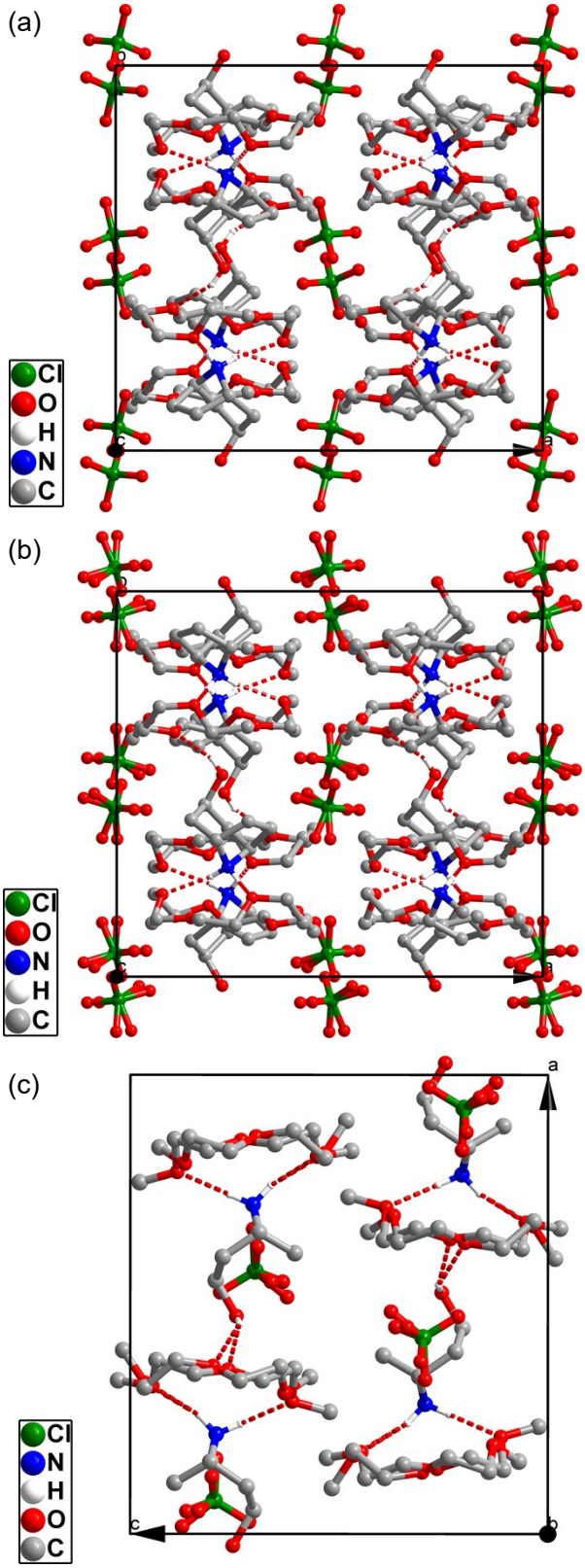

Figure S6. The crystallographic packing diagrams of **1** viewed along the *c*-axis in the LTP at 200 K (a), RTP at 293 K (b) and ITP at 365 K (c). Hydrogen atoms bonded to the C atoms were omitted for clarity. Dashed lines represent hydrogen bonds N–H···O and O–H···O.

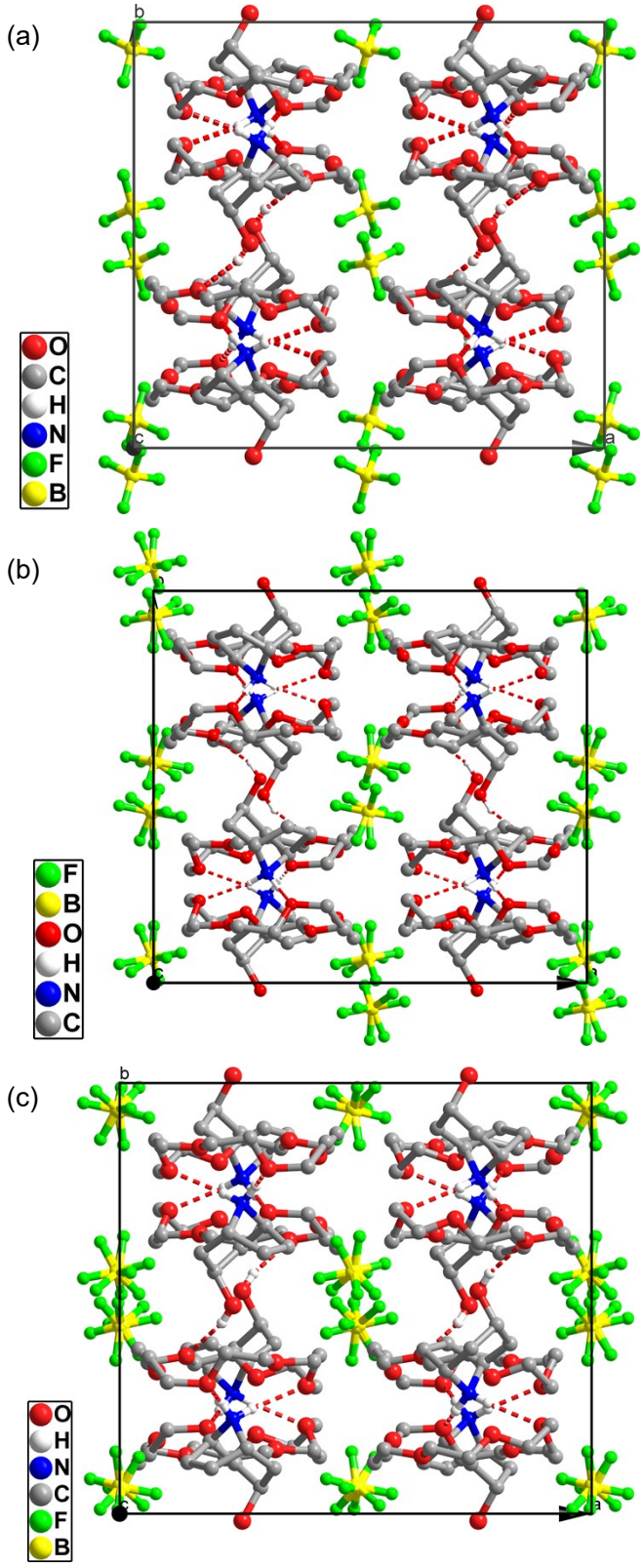

Figure S7. The crystallographic packing diagrams of **2** viewed along the *c*-axis in LTP at 173 K (a), RTP at 293 K (b) and at 350 K (c). Hydrogen atoms bonded to the C atoms were omitted for clarity. Dashed lines represent hydrogen bonds N–H···O and O–H···O.

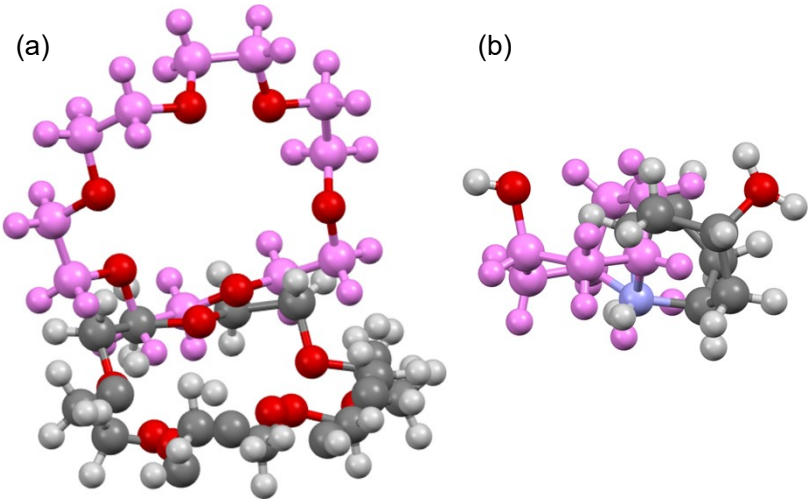

Figure S8. The conformational change of crown ether (a) and NRT (b) moiety in phase-I (carmine) and phase-III (gray) of **1** by providing an overlapping molecular image using mercury program.

IR and Raman spectroscopy characterization. IR spectra of the title compound were recorded on a Perkin-Elmer spectrum 2000 operating at 4 cm^{-1} resolution. Variable-temperature Raman measurements were carried out in a HORIBA equipped with a 50× (0.75 N.A.) objective with an excitation wavelength of 532 nm using a laser power < 0.1 mW to avoid the damage of the samples during the measurement.

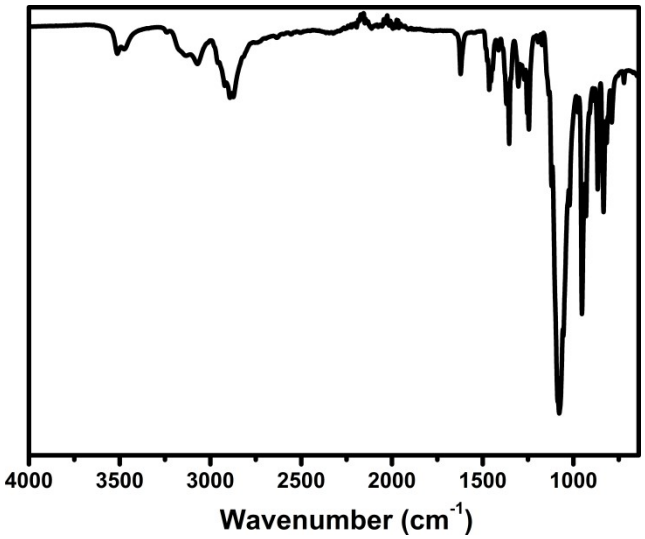

Figure S9. IR spectrum of **1**. The main peaks at 2894 are tentatively assigned the $\delta(CH_2)$ and at 1078 cm^{-1} are tentatively assigned the $\nu(ClO_4)$ and ν(C-O).

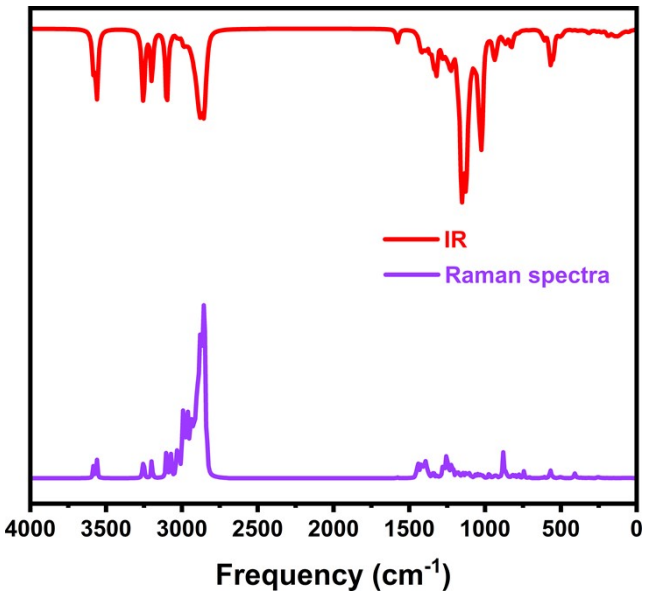

Figure S10. Calculated IR spectrum and Raman spectra of **1**. The main peaks at 2894 cm^{-1} are tentatively assigned the $\delta(CH_2)$ and at 1078 cm^{-1} are tentatively assigned the $\nu(ClO_4)$ and ν(C-O).

Table S2. Measured and calculated vibration wavenumbers (cm^{-1}) of **1** and proposed assignments of the observed Raman and IR bands.

Observed wavenumbers (cm^{-1})		Calculated wavenumbers (cm^{-1})	Proposed assignments
Raman	IR		
77	-	65	$\tau(CH_2)$ twisting
159	-	143	ω(C-O-C) wagging, $\omega(CH_2)$ wagging
223	-	198	ω(C-O-C) wagging
268	-	255	$\omega(CH_2)$ wagging
326	-	325	$\omega(CH_2)$ wagging
383	-	389	$\omega(CH_2)$ wagging
404	-	432	ω(Cl-O) wagging
459	-	447	$\omega(CH_2)$ wagging
524	-	523	$\omega(CH_2)$ wagging, $\omega(NH_2)$ wagging
568	-	581	δ(C-O) stretching
585	-	594	(C-O-C) bending
625	-	642	ω(OH) wagging
757	753	752	$\tau(CH_2)$ twisting
791	788	784	$\tau(CH_2)$ twisting
809	816	815	$\tau(CH_2)$ twisting
830	834	825	$\tau(CH_2)$ twisting
869	866	873	$\omega(CH_2)$ wagging
889	887	889	$\omega(NH_2)$ wagging
910	909	906	$\omega(CH_2)$ wagging, $\omega(NH_2)$ wagging
934	931	927	δ(ClO) stretching, $\omega(CH_2)$ wagging, $\omega(NH_2)$ wagging
979	976	985	$\omega(CH_2)$ wagging, $\omega(NH_2)$ wagging
1025	1021	1024	δ(C-C) stretching

1091	1077	1075	$p(ClO_4)$ rocking
1124	1121	1120	$\omega(CH_2)$ wagging
1140	1136	1139	$\omega(CH_2)$ wagging, δ(C-O) stretching
1153	1173	1166	$\omega(CH_2)$ wagging, $\omega(NH_2)$ wagging
1200	1194	1181	$\tau(CH_2)$ twisting, δ(ClO) stretching
1216	-	1212	$\omega(CH_2)$ wagging
1245	1245	1147	$\omega(CH_2)$ wagging
1276	1272	1277	$\tau(CH_2)$ twisting
1287	1303	1294	$\omega(CH_2)$ wagging
1309	1354	1345	$\tau(CH_2)$ twisting
1439	1412	1412	$\delta(CH_2)$ scissoring
1464	-	1436	$\delta(CH_2)$ scissoring, $\omega(NH_2)$ wagging
1474	1464	1470	$\delta(CH_2)$ scissoring
1486	-	1491	$\delta(CH_2)$ scissoring
1527	-	1514	$\delta(CH_2)$ scissoring
2966	2958	2960	$\delta(CH_2)$ stretching
2980	-	2981	$\delta(CH_2)$ stretching
2995	-	2998	$\delta(CH_2)$ stretching
3013	-	3023	$\delta(CH_2)$ stretching
3037	-	3037	$\delta(CH_2)$ stretching
3071	3071	3123	$\delta(CH_2)$ stretching
3522	3475	3429	$\omega(NH_2)$ stretching
3739	3736	3747	v(OH) stretching

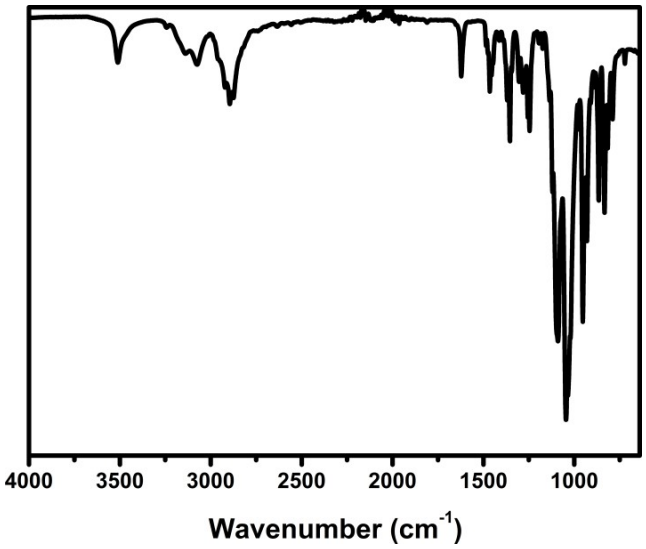

Figure S11. IR spectrum of **2**. The main peaks at 2895 cm^{-1} are tentatively assigned the $\delta(CH_2)$ and at 1045 cm^{-1} are tentatively assigned the $\nu(BF_4)$ and ν(C-O). Notation used: δ, stretching, ν, vibrations.

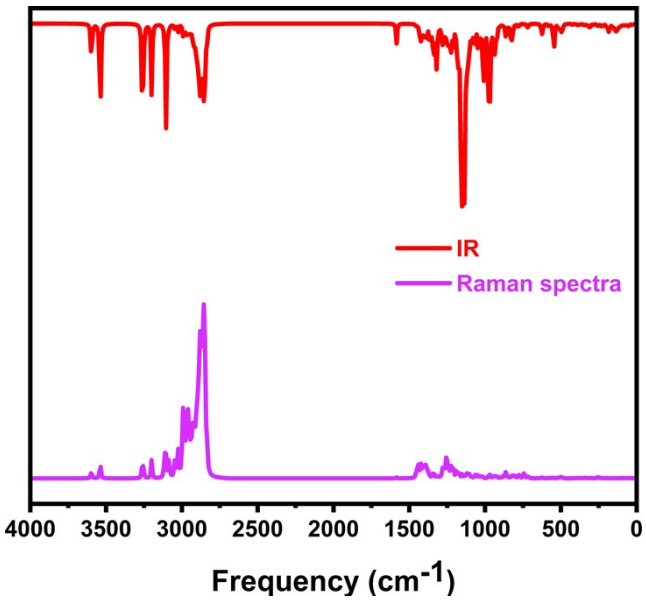

Figure S12. Calculated IR spectrum and Raman spectra of **2**. The main peaks at 2895 cm^{-1} are tentatively assigned the $\delta(CH_2)$ and at 1045 cm^{-1} are tentatively assigned the $\nu(BF_4)$ and ν(C-O). Notation used: δ, stretching, ν, vibrations.

Table S3. Measured and calculated vibration wavenumbers (cm^{-1}) of **2** and proposed assignments of the observed Raman and IR bands.

Observed wavenumbers (cm^{-1})		Calculated wavenumbers (cm^{-1})	Proposed assignments
Raman	IR		
76	-	77	τ(CH_2) twisting
107	-	109	τ(CH_2) twisting
167	-	169	ω(C-O-C) wagging
265	-	268	ω(CH_2) wagging
322	-	323	ω(CH_2) wagging
379	-	370	ω(CH_2) wagging, ω(NH_2) wagging
486	-	450	ω(CH_2) wagging, ω(NH_2) wagging
524	-	524	ρ(BF_4) rocking
566	-	546	ω(CH_2) wagging
585	-	583	(C-O-C) bending
631	-	655	ω(OH) wagging
725	721	752	τ(CH_2) twisting
766	789	760	δ(B-F) stretching
789	815	816	τ(CH_2) twisting
832	833	827	τ(CH_2) twisting
870	865	872	ω(CH_2) wagging
887	887	890	δ(C-N) stretching
911	909	912	ω(CH_2) wagging, δ(C-C) stretching
933	953	927	ω(CH_2) wagging, ω(NH_2) wagging
979	976	985	ω(CH_2) wagging, ω(NH_2) wagging
1022	1021	1021	δ(C-C) stretching, ω(BF) wagging
1047	1045	1060	ω(BF) wagging, ω(NH_2) wagging
1090	1090	1091	ω(CH_2) wagging, ω(NH_2) wagging
1124	1120	1123	ω(CH_2) wagging
1140	1136	1141	ω(CH_2) wagging, δ(C-O) stretching
1152	-	1159	ω(CH_2) wagging, ω(NH_2) wagging
1177	1174	1178	τ(CH_2) twisting, τ(NH_2) twisting
1196	1194	1197	ω(CH_2) wagging, δ(BF) stretching
1245	1246	1145	δ(C-O) stretching
1274	-	1276	τ(CH_2) twisting
1285	1281	1287	ω(CH_2) wagging
1306	1306	1308	ω(CH_2) wagging
-	1354	1347	τ(CH_2) twisting, δ(C-O) stretching
1411	1413	1412	ω(CH_2) wagging
1453	-	1453	δ(CH_2) scissoring
1463	1466	1461	δ(CH_2) scissoring, ω(NH_2) wagging
1474	1475	1474	δ(CH_2) scissoring
1486	1487	1491	δ(CH_2) scissoring
1527	-	1514	δ(CH_2) scissoring

2965	-	2981	$\delta(CH_2)$ stretching
2997	3002	2996	$\delta(CH_2)$ stretching
3018	-	3020	$\delta(CH_2)$ stretching
3041	-	3040	$\delta(CH_2)$ stretching
3077	3074	3078	$\delta(CH_2)$ stretching
3139	3138	3138	$\omega(NH_2)$ stretching
3247	3242	3248	$\omega(NH_2)$ stretching
3512	3511	-	$\omega(NH_2)$ stretching
3724	3724	3725	δ(OH) stretching
3786	3784	3786	δ(OH) stretching

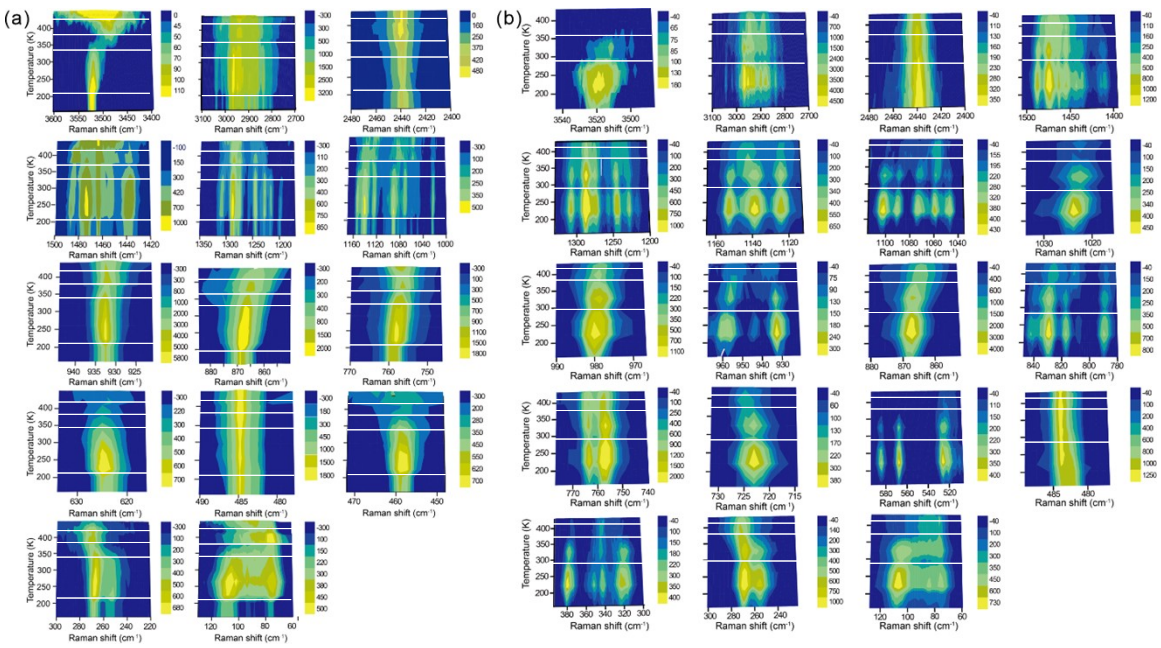

Figure S13. Temperature-dependent Raman spectra for **1** (a) and **2** (b) crystals in the range from 60 to 3900 cm^{-1}. The white dashed line indicates the phase transition location.

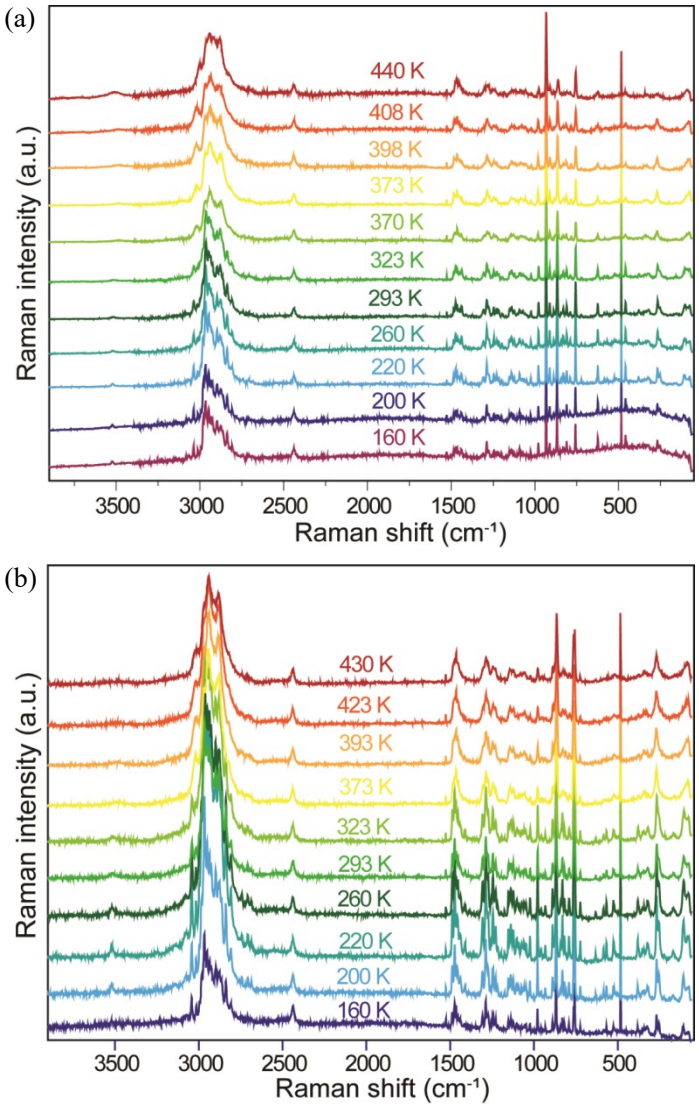

Figure S14. Raman spectra in the 60-3900 cm^{-1} region for **1** (a) and **2** (b) at different temperature.

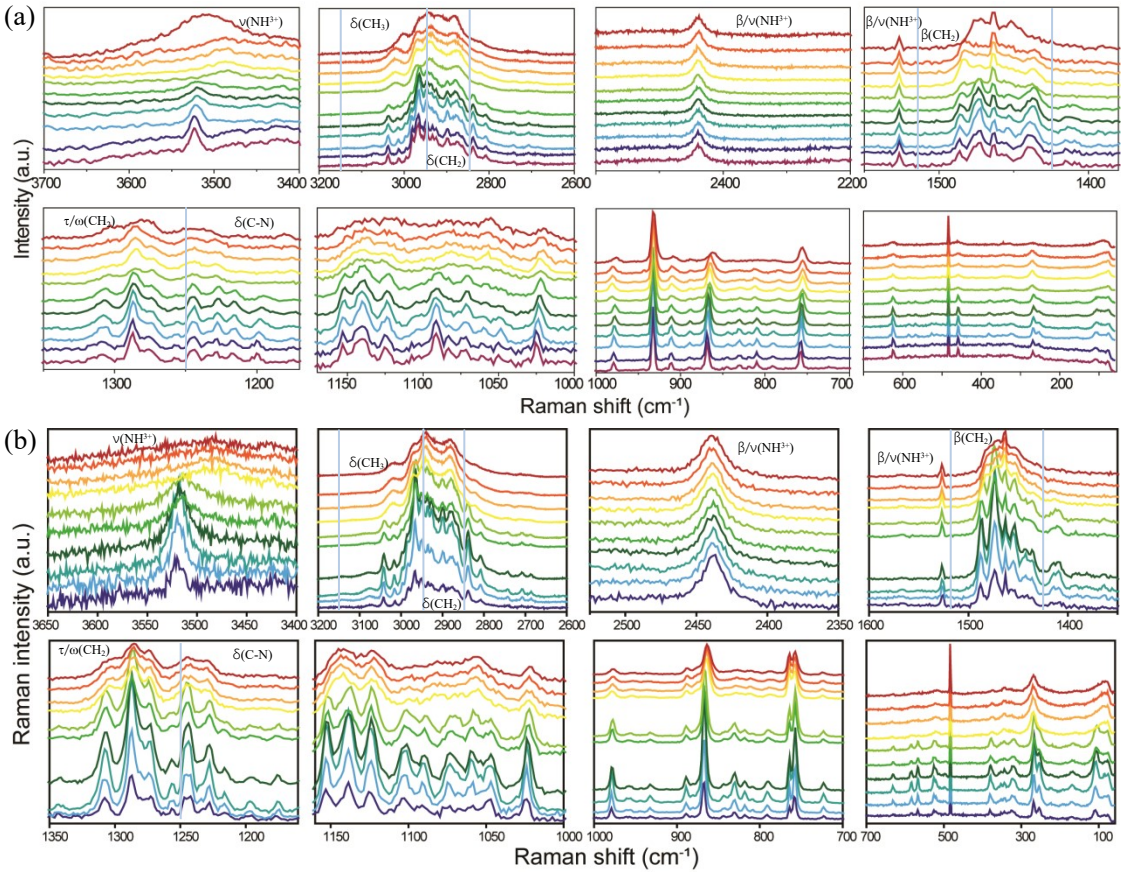

Figure S15. Raman modes for **1** (a) and **2** (b) at different temperature. Notation used: δ, stretching, β, bending; τ, twisting; ω, wagging, and ν, other vibrations.

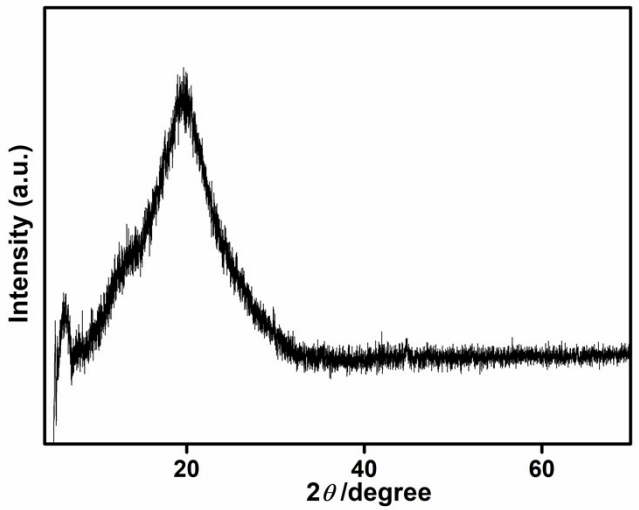

Figure S16. The powder X-ray diffraction of **2** at 430 K.

References

1. O. V. Dolomanov, L. J. Bourhis, R. J. Gildea, J. A. Howard and H. Puschmann, *J. Appl. Crystallogr.*, 2009, **42**, 339-341.
2. G. Sheldrick, *SHELXL-97, program for X-ray crystal structure refinement. University of Göttingen, Germany Göttingen*, 1997.
3. A. SIR92, *Altomare, G. Cascarano, C. Giacovazzo, A. Guagliardi, MC Burla, G. Polidori, MJ Camalli, J. Appl. Crystallogr.*, 1994, **27**, 435-436.